Engineering Geology 178 (2014) 109–120

Contents lists available at ScienceDirect

Engineering Geology

journal homepage: www.elsevier.com/locate/enggeo

Characterization of bi-planar and ploughing failure mechanisms in footwall slopes using numerical modelling

Mohsen Havaej [a,*], Doug Stead [a], Erik Eberhardt [b], Brendan R. Fisher [b,c]

[a] Simon Fraser University, Burnaby, British Columbia, Canada
[b] University of British Columbia, Vancouver, British Columbia, Canada
[c] Fisher & Strickler Rock Engineering, Radford, VA, USA

ARTICLE INFO

Article history:
Received 21 December 2013
Received in revised form 20 May 2014
Accepted 4 June 2014
Available online 14 June 2014

Keywords:
Footwall slope
Bi-planar failure
Ploughing failure
FDEM
DEM
Brittle fracture

ABSTRACT

Footwall slopes refer to unbenched rock slopes in which the slope face is parallel to a set of persistent discontinuities (e.g. bedding planes, foliation, faults). These are commonly encountered in weak, thinly bedded, orthogonally jointed, sedimentary rock sequences. Common failure mechanisms include bi-planar failures where shallow dipping crosscutting structures daylight near the slope toe, enabling sliding to occur along steep dipping bedding planes. In the absence of crosscutting structures, failure occurs through deformation and rock mass yielding involving the formation of inter block shear and toe breakout surfaces. Because of the complexity of the toe breakout mechanism, evaluation methods are not well understood. An improved understanding of the failure mechanism, the role of adverse discontinuities, and characterization of the discontinuity, intact rock and rock mass strength properties are key for a successful footwall stability analysis. This paper investigates the development of the inter block shear and toe breakout surfaces with three approaches: i) continuum-based frictional plasticity theory; ii) discontinuum-based distinct-element modelling with Voronoi tessellation using the commercial software UDEC; and iii) hybrid continuum/discontinuum finite-/discrete-element brittle fracture modelling using the commercial software ELFEN. Numerical simulations using ELFEN and UDEC demonstrated a good agreement with frictional plasticity theory. Ploughing failure of footwall slopes is also evaluated, specifically the influence of cross-cutting discontinuity dip angle relative to the slope face. The effects of different geometrical parameters (e.g., slope angle and depth/height ratio) on bi-planar and ploughing failure are assessed using a sensitivity analysis approach. A "Damage Intensity" parameter is introduced and used to quantify damage in the numerical simulations using ELFEN.

1. Introduction

In the surface mining of metallurgical coal, where the strata have undergone tectonic folding, slopes are often excavated parallel to the strata dip in synclinal and anticlinal structures forming extensive, high and unbenched footwall slopes (Stead and Eberhardt, 1997). Footwall slopes, also referred to as dip slopes, are encountered in other mine and engineered slopes (e.g., road cuts) where instability is structurally controlled, typically by a joint set, fault or weak zone parallel or sub-parallel to the slope (Konietzky, 2004; Fisher, 2009; Alejano et al., 2011). These authors classify the most commonly encountered footwall failure mechanisms into fully and partially joint-controlled (or rock mass-controlled in the case of the latter) and describe limit equilibrium and numerical approaches for obtaining the factor of safety of bi-planar and ploughing failures. In fully joint-controlled failure mechanisms, stability is primarily governed by the strength of the discontinuities. In the absence of fully persistent discontinuities enabling kinematic release, a more complex failure can occur through sliding along the major geological discontinuities, step-path failure and shearing through intact rock (i.e., rock mass failure).

Hawley et al. (1986) studied the failure modes in western Canadian surface mines and developed limit equilibrium analysis techniques for different modes of failure. Stead and Eberhardt (1997) also reviewed the different failure modes in surface coal mine footwall slopes, discussing the key factors that affect their stability. Based on the analysis of footwall slopes at the Quintette Coal Mine in northern British Columbia and Westfield Opencast Coal Mine in the UK, they introduced a numerical approach to analyse different footwall failure modes using continuum (finite difference) and discontinuum (distinct element) methods. Fisher and Eberhardt (2007) carried out similar distinct-element modelling together with limit equilibrium analyses to provide practical recommendations for the stability evaluation of footwall slopes. Tannant and LeBreton (2007) surveyed a steep footwall slope at Grande Cache coal mine using terrestrial photogrammetry before and after its failure to investigate slope deformation and ultimate failure

* Corresponding author at: Earth Sciences Department,Simon Fraser University, Burnaby, BC, Canada.

http://dx.doi.org/10.1016/j.enggeo.2014.06.003
0013-7952/

mechanisms. They conducted simple force equilibrium analyses to back-analyse the shear strength properties of the slip surface. Bahrani and Tannant (2011) also investigated this failure. They used photogrammetry to generate failure surface roughness profiles to calculate the dilational component of the shear strength of the failure surface.

Based on these earlier studies, it is clear that the stability of footwall slopes is mainly controlled by the shear strength of the dominant, slope parallel discontinuities upon which sliding may occur. However, because these discontinuities are parallel to the slope and do not 'daylight' in the slope face, they are not considered in a simple planar/wedge kinematic evaluation such as that provided by Hoek and Bray (1981). Nevertheless, failure may still develop depending on the orientation of other cross-cutting discontinuities and rock mass shear strength, and involve bi-planar, buckling, ploughing and step-path failure modes (Stead and Eberhardt, 1997). Thus, to study the stability of high footwall slopes, it is necessary to consider the interaction between existing discontinuities (e.g. bedding planes and cross-cutting joints), intact rock bridges and rock mass strength. Development in sophisticated numerical codes and increasing computing power has made it possible to consider the complex interaction between intact rock, discontinuities, in situ stress, groundwater, dynamic loads, etc. In this study, analytical and advanced numerical modelling approaches are used to investigate the role of brittle fracturing in the development of bi-planar and ploughing failure modes in footwall slopes.

2. Bi-planar failure of footwall slopes

Bi-planar failure occurs when a rock mass slides sub-parallel along persistent discontinuities, such as a bedding plane or fault, with kinematic release enabled through shearing along a secondary shallow dipping discontinuity dipping out of the slope face (Figure 1). A review of the geotechnical literature suggests that bi-planar footwall slope failures are most prevalent in weaker, bedded sedimentary rock sequences (e.g., flysch). Footwall slopes are often associated with anticlines, synclines, and homoclines. Although less common, footwall slopes may also form where faults, shears, or lithologic boundaries occur parallel to an excavated slope. A good example is that presented by Behrens da Franca (1997). He completed a detailed back analysis of a mine slope that was excavated exposing a soft hematite layer with a deposit of itabirite located approximately 30 m behind and parallel to the slope face. At the contact of the hematite and itabirite, there was a thin layer of soft itabirite or leached iron formation which acted as the slope parallel sliding surface causing failure. Bi-planar failures have been reported for natural slopes (e.g. Chen, 1992; Eberhardt et al., 2005). These can develop due to weathering of weaker shale beds or other factors that contribute to progressive failure.

2.1. Different modes of bi-planar failure

Stead and Eberhardt (1997) illustrated variations of bi-planar failure mechanism based on a survey of UK footwall failures and a review of the relevant literature:

2.1.1. Sliding on bedding planes and a basal surface with active/passive zones

The most common mode of bi-planar failure forms when a low angle daylighting thrust plane or cross-cutting joint forms a basal release surface (Stead and Eberhardt, 1997). This type of failure involves an active–passive wedge failure mechanism. Fig. 2 schematically shows a bi-planar failure and location of the active and passive blocks, separated by a Prandtl wedge transition zone. Kvapil and Clews (1979) describe this transition zone as being characterized by severe fracturing and secondary shearing of the rock mass as the forces are transmitted from the active to passive block. This may be observed as large transverse displacements (or inter block shearing) and bulging of the rock mass within the transition zone. In contrast, very little rock mass deformation occurs in the active zone. The majority of the deformation is concentrated along the slope-parallel sliding surface that serves as the release surface in the upper part of the slope. Likewise, there is minimal disturbance of the rock mass within the passive zone, although more than in the active zone. Clearly the rock mass strength within the Prandtl wedge and at the slope toe has an important influence on the amount of movement and ultimately the stability of the rock slope. The strength along the rupture surface in the upper slope is also important as it controls the amount of driving force transmitted to the Prandtl wedge and passive zone below. Stead and Eberhardt (1997) highlighted the work undertaken by Brawner et al. (1971) in which they recognized and proposed methods of analysis for bi-planar failures involving bedding and low angle basal surfaces. They derived stability charts for estimating the allowable footwall slope height as a function of geometrical characteristics of the slope; e.g., bedding angle, bedding thickness, cross-cutting joint orientation, and bedding/joint friction angle.

2.1.2. Persistent basal surface and inter block shear surface

The simplest toe breakout and inter block shearing mechanism involves sliding along the slope parallel sliding surface with a

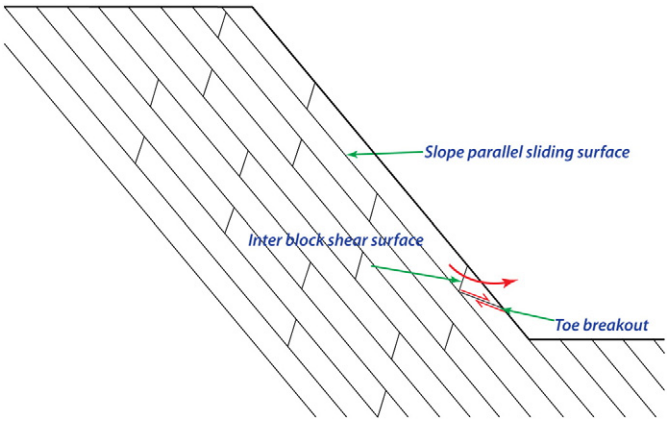

Fig. 1. Bi-planar failure of footwall slopes.

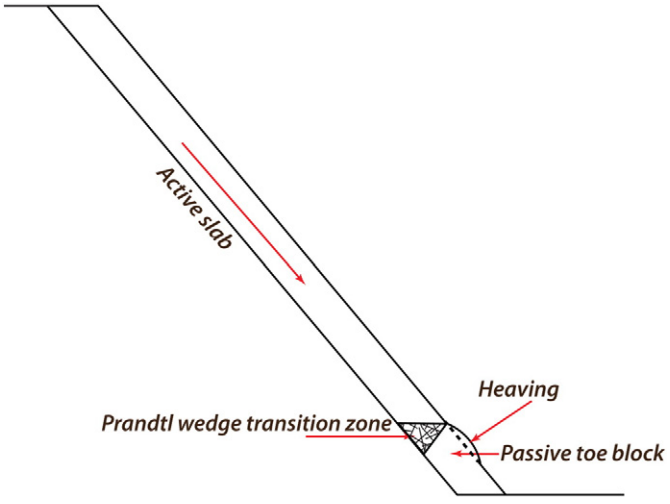

Fig. 2. Location of the Prandtl wedge in a bi-planar footwall failure (modified after Stead and Eberhardt (1997)).

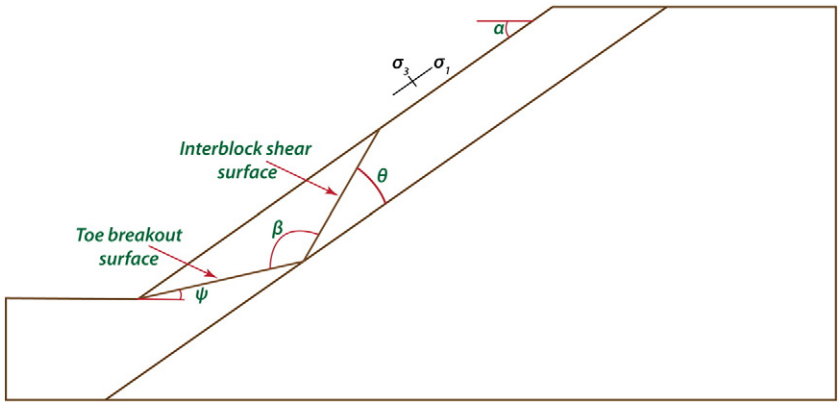

Fig. 3. Parameters used in the frictional plasticity approach.

persistent joint dipping out of the slope and a joint (or other persistent discontinuity) dipping steeply into the slope separating the active/passive wedges and providing kinematic release of the slope (Nathanail, 1996). The slope and structural geology model required for this type of failure is shown in Fig. 1 where it could be envisioned that the inter block shear and toe breakout surfaces both consist of through-going discontinuities. This model illustrates that in addition to the basal shear surface, inter block shear is required for slope release.

2.1.3. Step-path failures

A step-path (or rock mass) failure occurs where toe break out and/or inter block shear develops through the combined sliding along non-persistent joints and failure of intact rock bridges. Jennings (1970) presented a detailed limit equilibrium model for estimating the stability of a slope where step-path failure may occur. The model effectively uses a weighted average of the shear strength of the joints and the shear strength (or tensile strength) of the intact rock through which the sliding surface develops. More recently, the Hoek–Brown failure criterion presents a means to weight the combined influence of intact rock and non-persistent joint strength as an equivalent continuum rock mass strength (Hoek and Brown, 1997; Hoek et al., 2002; Carvalho et al., 2007). Giani (1992) provides a detailed account of a footwall slope back analysis where the toe breakout was modelled using the Hoek–Brown failure criterion. It should be noted, though, that the treatment of the step-path problem as an equivalent continuum neglects the important kinematic and directional controls that exist where the discontinuities are of moderate persistence. In such cases, the equivalent continuum approach may only apply to the rock mass strength of the rock bridges to account for smaller-scale discontinuities that serve to weaken the rock bridge.

2.1.4. Buckling model

A footwall buckling failure is characterized by bending and sliding (flexural slip) of the outermost layers above the toe of the slope as a toe breakout surface or inter block shear develops. Buckling prior to kinematic release in layered sedimentary rock has been reported along the Yalong River, China (Wang et al., 1992), Yangtze River, China (Li et al., 1992) and within several coal mines in Canada and the UK (e.g., Scoble, 1981; Cruden and Masoumzadeh, 1987; Stead and Eberhardt, 1997). Jin et al. (1992) and Li et al. (1992) both provide details of a friction model analysis of these bi-planar slope failures which occurred over a 50-month period. The model was constructed to represent bedded strata in which bedding was inclined at an angle

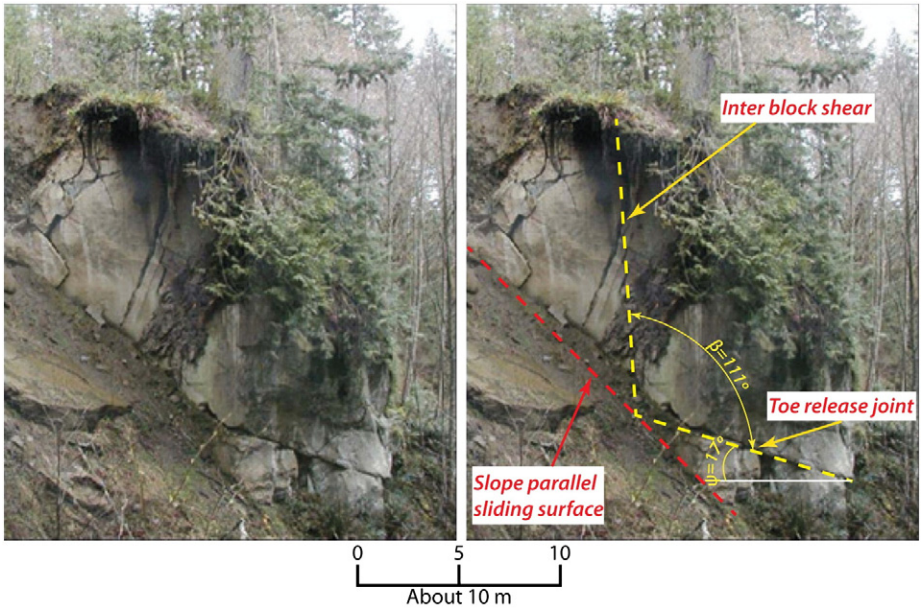

Fig. 4. Bi-planar failure in sedimentary rock.

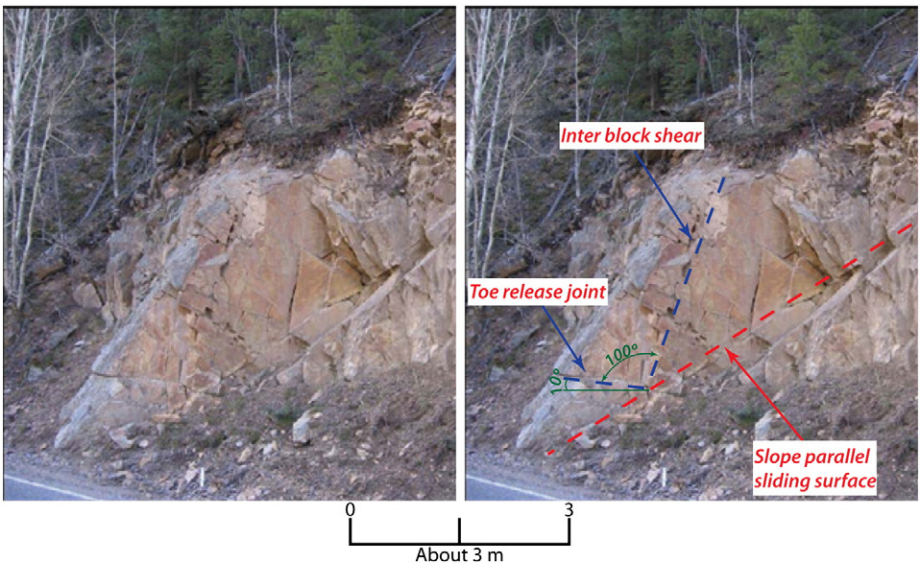

Fig. 5. Bi-planar failure in metamorphic rock.

greater than the residual friction angle. They observed progressive failure of the model slope with the first indications of failure being buckling of the outermost layers. The deformations advanced further behind the slope face followed by bi-planar shearing across bedding. This model suggests that one of the first indications of bi-planar slope failure may be bulging at the slope toe.

2.2. Treatment of toe breakout using a frictional plasticity approach

Limit equilibrium represents the most common method for estimating the stability of footwall slopes where bi-planar failure is considered. Brawner et al. (1971) and Stimpson and Robinson (1982) provide methods where the toe breakout surface is varied while the inter block shear is assumed sub-normal to the slope face. This failure mechanism is the same as shown in Fig. 1 with the inter block shear surface assumed sub-normal to bedding. No consideration is given to the strength of the inter block shear. Hawley et al. (1986) provide similar solutions where the inter block shear is sub-normal to the slope face and shear strength parameters are assigned to the inter block shear. Clearly the assumptions used to generate these solutions apply to very specific geological conditions.

Where there are no clear planes of weakness forming either the toe breakout surface or inter block shear (or both), brittle fracturing must occur through the rock mass. Limit equilibrium methods adopt a holistic approach, which require generalizing assumptions with regard to the nature of the rupture surface and failure kinematics. To counter these deficiencies, frictional plasticity theory was examined to develop a better mechanistic understanding regarding the development of toe release and inter block shear surfaces.

Quick scoping calculations immediately suggest that the location of the inter block shear may be described by plasticity theory where expected failures are relatively shallow and the major principal stress (σ_1) is parallel to the slope face. These calculations are based on the Mohr–Coulomb failure hypothesis relating localization and the shear failure surface that develops at an angle (θ) to the plane of the major principal stress (σ_1) as a function of the friction angle of the material (φ) (Eq. 1). The practical importance of this is that because σ_1 within footwall slopes is oriented parallel to the slope face, and therefore bedding, it becomes possible to calculate the orientation θ of the shear

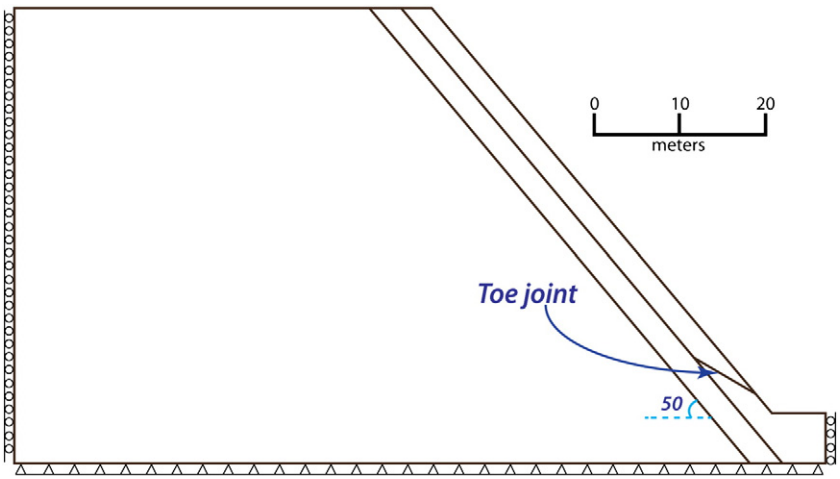

Fig. 6. Assumed geometry for FDEM modelling of bi-planar failure.

Table 1
Intact rock strength parameters.

Property	Value
USC (MPa)	30
Young's modulus (GPa)	15
Poisson's Ratio	0.25
Density (kg/m^3)	2500
Friction angle (°)	45
Tensile strength (MPa)	2
Cohesion (MPa)	5

failure surface at the toe along which toe breakout should develop. The angle θ also describes the orientation of the inter block shear that develops to accommodate slippage between the active and passive blocks and facilitates sliding along the toe breakout surface (Eq. 2).

$$\theta = 45 - \frac{\varphi}{2} \quad (1)$$

$$\psi = \alpha + \frac{\varphi}{2} - 45 \quad (2)$$

$$\beta = 90 + \theta \quad (3)$$

where ψ is the toe breakout angle and α is the slope angle, both measured from horizontal, and β is the angle between the inter block shear and the toe breakout surface (Figure 3). The relationship above is unaffected by the presence of orthogonal cross-jointing as the orientation of σ_1 (i.e., parallel to slope/bedding and perpendicular to the cross joints) means that no shear stresses develop along the cross-joints; the normal stress acting on the cross joints is equal to σ_1.

Figs. 3 and 4 show examples of bi-planar rock slope failures where the toe breakout surface and inter block shear correspond to those predicted by frictional plasticity theory. The sedimentary rock mass in Fig. 4 is orthogonally jointed and a tension crack can be seen as forming behind the inter block shear normal to the slope coincident discontinuity. The orthogonal joint opened in tension as the inter block shear initiated and propagated through the rock. The slope in Fig. 5 involving metamorphic rock similarly shows the inter block shear developing through the rock mass as a rock mass failure.

3. Numerical modelling of bi-planar failure of footwall slopes

In the absence of inter block shear and toe break-out surfaces coinciding with fully persistent discontinuities, bi-planar failure of footwall slopes must occur through failure of intact rock bridges and rock mass shear providing kinematic release. Thus, numerical simulation of this type of failure requires the use of a code that allows for fracture initiation and propagation. The two dimensional hybrid finite/discrete element (FDEM) code ELFEN (Rockfield., 2009) was used in this study to investigate the formation of inter block shear surfaces, active–passive transition zones, and toe breakout. The code has been verified against several rock engineering case studies (e.g., Elmo and Stead, 2010 and Vyazmensky et al., 2010). Stead et al. (2006) suggest three levels of sophistication in slope stability problems in which hybrid numerical analyses fall in the third level of complexity. FDEM codes such as ELFEN have the capability of modelling fracture propagation and fragmentation of a jointed and bedded rock mass based on fracture mechanics principles

Table 2
Discontinuity strength parameters.

Discontinuity	K_n (GPa/m)	K_s (GPa/m)	Friction angle (°)	Cohesion (MPa)
Crosscutting joint	10	1	40	0
Beddings plane	10	1	30	0

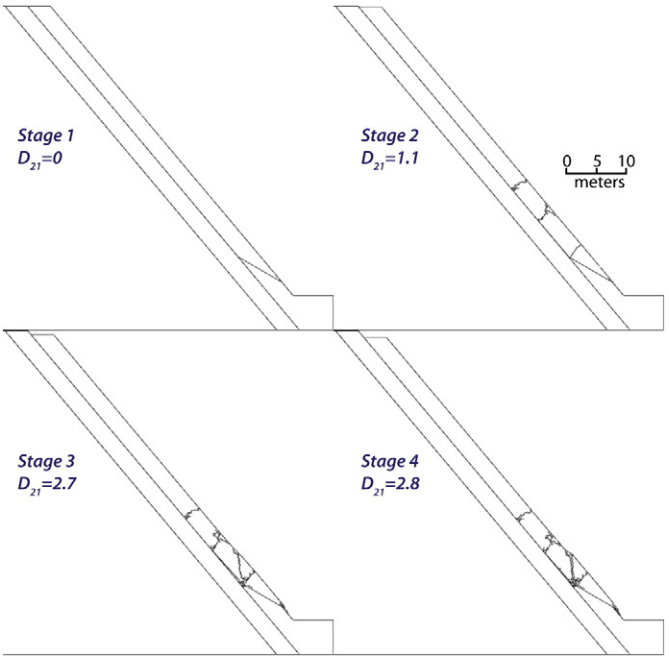

Fig. 7. ELFEN simulation of a 50 m high footwall slope with a bi-planar (active–passive) failure surface showing stages of fracture development leading to slope failure.

(Stead et al., 2006). ELFEN uses a finite element mesh to model the intact joint bounded blocks and discrete elements to model joint and fracture contacts and their behaviour (Stead et al., 2006).

A new approach is suggested to quantitatively evaluate progressive failure in a footwall slope. A damage intensity parameter D_{21} is proposed equal to the ratio of the total length of generated cracks to the sampling area, Eq. 4 (Gao, 2013; Hamdi et al., 2013). Gao (2013) used D_{21} to characterize damage in simulation of roof failure in underground coal mines. At the laboratory scale, Gao (2013) and Hamdi et al. (2013) utilized D_{21} to quantify damage in 2D/3D numerical simulation of unconfined compression and Brazilian tests. In this paper, the progressive failure of the bi-planar and ploughing models will be quantified using D_{21}. The total area of the footwall slab in the models is considered as the sampling area for damage quantification in Eq. 4. A shear strength

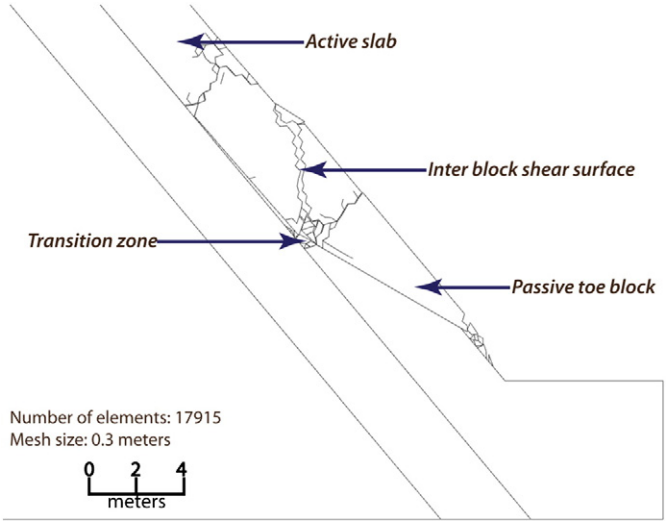

Fig. 8. Inset showing location of the transition zone (between the two fracture surfaces), delimiting the active and passive block, $D_{21} = 2.8$.

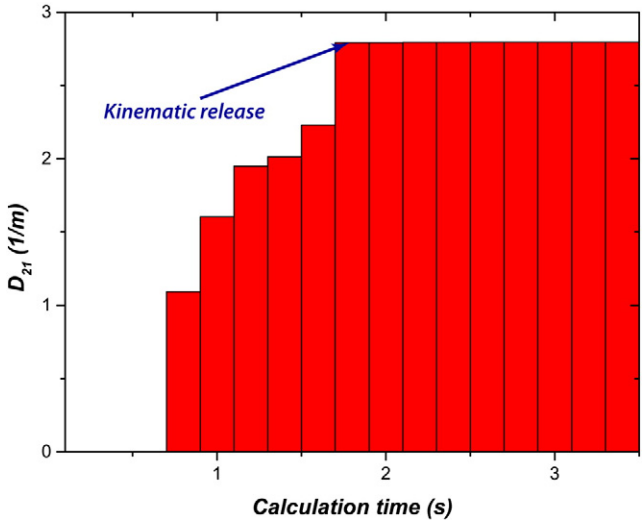

Fig. 9. Damage intensity, D_{21}, vs. ELFEN simulation time.

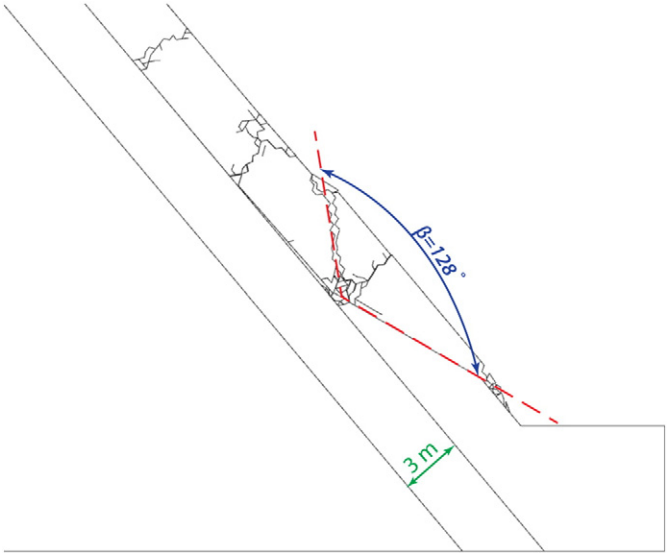

Fig. 11. The angle between the toe joint and inter block shear surface.

reduction technique is utilized to compute the safety factor of each model and compare with the calculated damage.

$$D_{21}\left({}^{m}/_{m^2}\right) = \frac{\text{total damage length (m)}}{\text{sampling area } (m^2)}. \quad 4$$

Numerical simulations in this paper are conducted using the footwall slope geometries published in Alejano et al. (2011). The analysis is conducted for a 50 m slope dipping 50°, formed by 3 m spaced bedding planes dipping parallel to the slope face (Figure 6). The strata are crosscut by a toe joint dipping 30° out of the slope. The lateral boundaries are fixed with zero displacement constraints in the horizontal direction and the bottom boundary is fixed in both horizontal and vertical directions. The intact rock and discontinuity properties used, presented in Tables 1 and 2, were selected from the literature (Stead and Eberhardt, 1997; Alejano et al., 2011) as being representative of moderately strong sedimentary rocks.

Fig. 7 illustrates an ELFEN simulation showing the development of brittle fracturing within the footwall slope providing kinematic release and subsequent slope failure. Development of orthogonal tensile fractures in the lower half of the slab is evident at stage 2 which is caused by sliding and bending of the slab as it moves on the cross-cutting toe joint with a calculated damage intensity, D_{21}, value of 1.1 (m/m^2). The modelling results show development of an inter block shear surface and a transition zone between the active and passive blocks at stage 3 with an increase in damage intensity to 2.7 (m/m^2) (Figure 8). Similar results have also been obtained in recent lattice spring Slope Model (Itasca, 2010) simulations of a bi-planar slope geometry by Tuckey et al. (2012). Damage intensity vs. simulation time is illustrated in

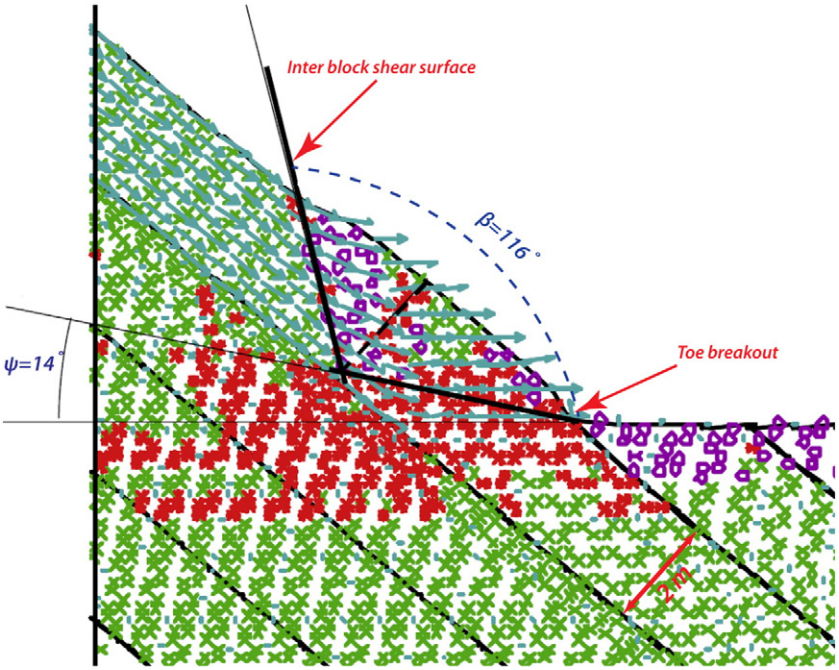

Fig. 10. UDEC model of a partially joint-controlled, bi-planar failure, with passive block translation (modified after Alejano et al., 2011).

Table 3
Micro-properties of Voronoi blocks in UDEC model.

Contact properties	Values
Normal stiffness of contacts, k_n (GPa/m)	8.4
Shear stiffness of contacts, k_s (GPa/m)	3.4
Contact cohesion, c^{cont} (MPa)	6.5
Contact friction angle, φ^{cont} (°)	18
Contact tensile strength, σ_t^{cont} (MPa)	3

Table 4
The influence of toe release joint dip on bi-planar failure of footwall slopes.

Model	Basal surface dip (°)	SRF	D_{21}
Base model	30	0.8	2.8
mode 1	25	0.85	2.6
mode 2	20	1	0.4

Fig. 9 showing a continuous increase in D_{21} up to the point that kinematic release is fully provided.

3.1. Application of frictional plasticity theory

As previously stated, the assumed geometry in this paper is based on Alejano et al. (2011) who used frictional plasticity theory originally suggested by Fisher and Eberhardt (2007) to calculate toe breakout in footwall slope modelling using UDEC (Itasca, 2012). Fig. 10 shows their simulated toe breakout angle and the angle between the toe breakout surface and the inter block shear surface. In their modelling, Ψ is 14° and β is 116°. Using Eqs 1, 2 and 3, calculated values for Ψ and β are 13° and 118° respectively, providing good agreement between the two approaches. A similar approach has been used in this paper. Since in the current numerical model a predefined toe joint is assumed, the toe breakout angle is not evaluated. As illustrated in Fig. 11, the results of ELFEN modelling are in a good agreement with the UDEC results presented by Alejano et al. (2011). Since the friction angle used in the ELFEN modelling is 45°, Eq. 3 returns a value of 113° for the angle between the toe breakout and internal shear surfaces. This compares to 128° produced by the ELFEN model (Figure 11).

The UDEC studies previously discussed (Stead and Eberhardt, 1997; Fisher and Eberhardt, 2007; Alejano et al., 2011) were carried out using a conventional approach in which footwall failure was modelled as the movement of slabs along slope parallel and cross-cutting discontinuities. Failure of the joint-bounded blocks was limited to elasto-plastic yield and large deformations, with no capability to simulate brittle fracture and fragmentation. Addition of a Voronoi tessellation generator to UDEC enables the user to create a network of polygons within the joint-bounded rock blocks that can be used to simulate failure of intact rock bridges through tensile/shear failure of contacts between the Voronoi blocks. Recent applications of UDEC Voronoi in rock mechanics have been described by several authors (e.g., Yan, 2008; Alzo'ubi, 2009; Kazerani and Zhao, 2010). At the laboratory scale, Alzo'ubi, et al. (2007) used UDEC Voronoi to simulate experiments conducted by Lajtai (1969) involving direct shear testing of joints. At the slope scale, the same authors re-analysed a planar failure with a discontinuous rupture surface previously investigated by Stead and Eberhardt (1997). They successfully used UDEC Voronoi to simulate the internal fracturing required for rock bridge failure and rupture surface development.

UDEC Voronoi is used in this research for simulating the bi-planar slope failure scenario previously analysed using ELFEN and frictional plasticity theory. In the footwall slope, where more fracturing and instability is expected, smaller Voronoi block sizes (0.5 m) are used. In the rest of the model, a Voronoi block size of 4 m is assumed. The Voronoi blocks themselves are assumed to be deformable. The input parameters for the UDEC model are the same as the parameters used in the ELFEN models (Tables 1 and 2). Micro-properties of the Voronoi contacts were selected based on calibrated UDEC Voronoi simulations of sandstone in a coal mine (Gao, 2013) and are presented in Table 3.

The results are presented in Fig. 12, and show tensile fracturing of the intact rock slab forming the inter block shear surface allowing kinematic release. The UDEC Voronoi simulation shows failure of the model through formation of active and passive blocks with a highly fractured transition zone between (Figure 12). The modelling results also show formation of the inter block shear surface as previously obtained in the ELFEN simulation and analysis using frictional plasticity theory.

3.2. Controls on bi-planar failure of footwall slopes

The importance of geometrical characteristics and the orientation of discontinuities on footwall slope failure were further investigated using ELFEN with a focus on the effect of both the toe joint dip angle and the bedding thickness to slope height ratio (D/H) on bi-planar failure. The model studied in the previous section is used for the parametric analysis and is referred to here as the "base model". To evaluate the stability of the slope a FDEM Strength Reduction Factor (SRF) for each model is calculated. History points are located at the slope crest where simulated displacements are recorded. The damage intensity, D_{21} is also determined for each numerical simulation as a measure of progressive brittle damage in the model.

3.2.1. Toe release joint dip angle

The base model, with 50° dipping bedding planes, includes a toe joint with a 30° dip to enable toe release. Keeping all other parameters constant, the toe joint inclination was decreased to 25° and 20°. Horizontal displacement of the slope crest is recorded to monitor footwall stability. Decreasing the dip from 30° to 25° does not change the overall stability of the model as the measured SRF value for both models are less than one (Table 4). Simulated displacements of the slope crest show an initial acceleration followed by a decrease in the rate of movements after 20 cm of slip for the model with a 25° toe joint (Figure 13). Damage intensity is slightly decreased suggesting that a certain degree of damage is required for failure to initiate (Table 4). When the dip of the daylighting toe joint is further reduced to 20°, the intensity of slope damage changes as does the stability of the slope (Table 4).

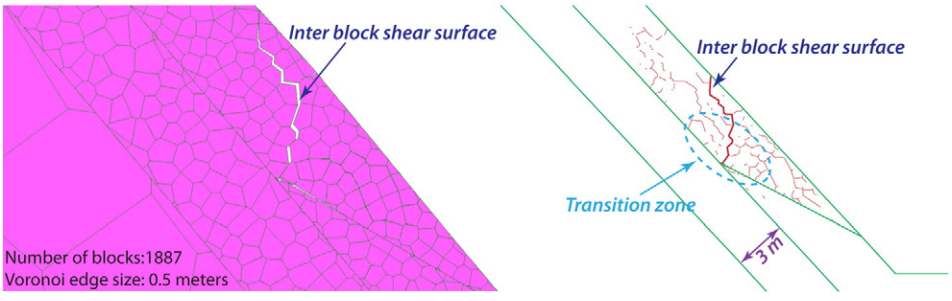

Fig. 12. UDEC Voronoi simulation of bi-planar failure shown in fig. 6, demonstrating development of inter block shear surface and highly fracture transition zone.

Minor fracturing occurs in the middle of the slab and perpendicular to it (Figure 14). However, displacements reach equilibrium after only a few centimetres of initial movement (Figure 13). The simulation results indicate that the increasing stability observed in the history plots is due to the decreased angle of the toe joint.

3.2.2. Bedding thickness to slope height (D/H) ratio

The effect of slope height on bi-planar failure of footwall slopes has been investigated in the literature (Hawley et al., 1986; Stead and Eberhardt, 1997; Stead et al., 2006; Fisher, 2009). An increase in slope height serves to increase the driving forces imposed on the passive block, which enhances the potential for plastic deformation and shear at the slope toe. In the case of convex slopes, an increase in slope height causes increased tensile fracturing in the most curved portions of the slope leading to buckling failure. From a structural geology perspective, increased slope height increases the probability of an adverse structure daylighting in the slope face (Stead and Eberhardt, 1997). Based on a survey of published literature on surface coal mines, Stead and Eberhardt (1997) note that slabs in footwall slopes generally range in thickness from 0.3 m to 10 m and stability increases with increase in bedding thickness. Fisher (2009) provided a review of footwall failure case histories in natural and engineered rock slopes (mostly within sedimentary lithologies) in which he reported the depths of failure to slope height ratios (D/H) for each case and suggested that the depth of failure is generally less than one third of the slope height. He also reported the trigger of failure for each case history including increase in water pressure, long-term creep, buckling at the toe, seismic acceleration and weathering. The sensitivity of the footwall models to the D/H ratio is hence investigated by gradually increasing the D/H ratio and observing the effect on the failure mechanism. The damage intensity (D_{21}) is almost the same for all the models with a SRF less than one (Table 5). The results show that stability of the footwall slope decreases with decreasing D/H ratio (Figure 15). For the unstable models, the failure mechanism is similar to the base model with sliding on the daylighting toe joint and bending of the slab causing fracturing perpendicular to the bedding.

4. Ploughing failure mechanism

Ploughing failure although not common, is a type of footwall slope failure which occurs when a sub-vertical discontinuity intersects steep bedding planes at the slope face (Figure 16). Ploughing occurs when an active slab sliding along the slope parallel bedding planes transfers driving forces to the passive slabs through the secondary steeply dipping discontinuity causing rotation of the passive slab out of the slope

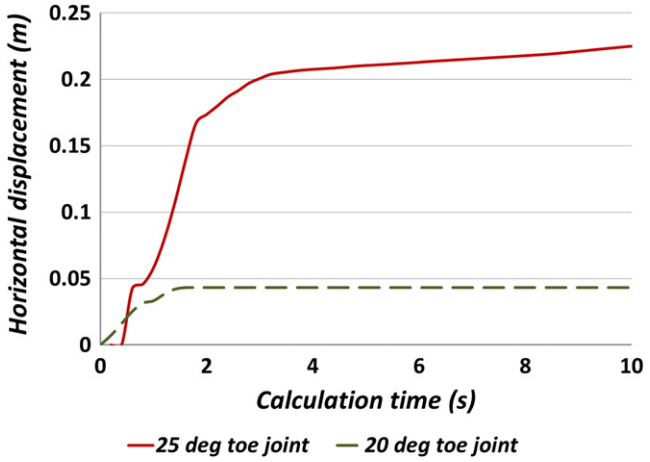

Fig. 13. Horizontal displacement vs. calculation time at the slope crest.

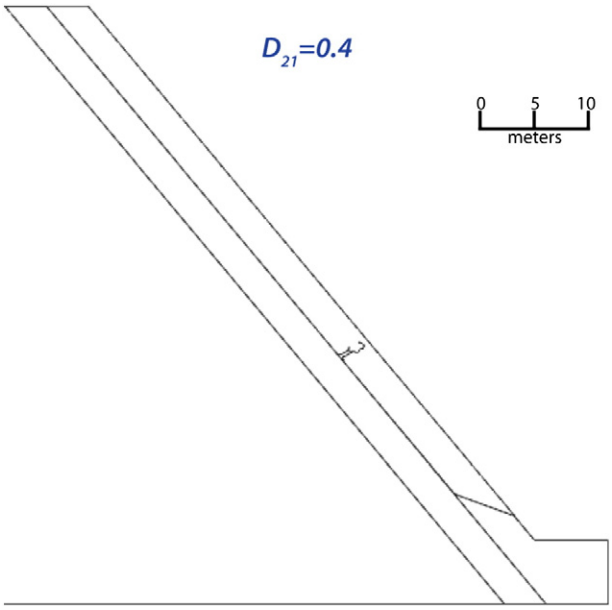

Fig. 14. Limited slope damage as a result of the decreased toe joint dip (20°) resulting in a stable footwall slope.

(Figure 16) (Hawley et al., 1986). This type of failure is unlikely to occur at the slope toe because the lower block is locked into place by the confinement created by the pit floor and overburden (Stead and Eberhardt, 1997). A limit equilibrium approach for analysing ploughing is presented by Hawley et al. (1986). Using simple geometry, they proposed an equation to calculate the maximum allowable slope height and suggested that the limit equilibrium results are particularly sensitive to the length of the toe block (passive slab). They recommended that a number of potential toe block geometries be assessed to determine the critical length of the toe block and hence, the critical slope height. Alejano et al. (2011) proposed a limit equilibrium approach to calculate the factor of safety considering both sliding and rotation of the passive block. They also applied a shear strength reduction (SSR) technique in UDEC to constrain the results of limit equilibrium analysis.

4.1. Ploughing analysis

A FDEM analysis using ELFEN with SSR was performed for a 50 m slope dipping at 60°, formed by 1 m thick slope parallel bedding planes (Figure 17). The slab is crosscut by a toe joint dipping normal to bedding and a secondary joint with the same properties that dips vertically forming a 30° angle with the bedding plane. The same boundary conditions and input properties (Tables 1 and 2) were used as for the bi-planar failure analysis. Similarly D_{21} is utilized for damage quantification and the SRF determined as a measure of model stability. Fig. 18 illustrates four stages of brittle fracture development within the slab. Failure starts with the active slab sliding on the bedding plane causing

Table 5
The effect of D/H ratio on bi-planar failure of footwall slopes.

Model	D/H	SRF	D_{21}
Base model	0.06	0.8	2.8
Model 1	0.07	0.85	2.6
Model 2	0.08	0.88	2.6
Model 3	0.09	0.95	2.7
Model 4	0.1	1	1
Model 5	0.12	1.03	0
Model 6	0.13	1.1	0

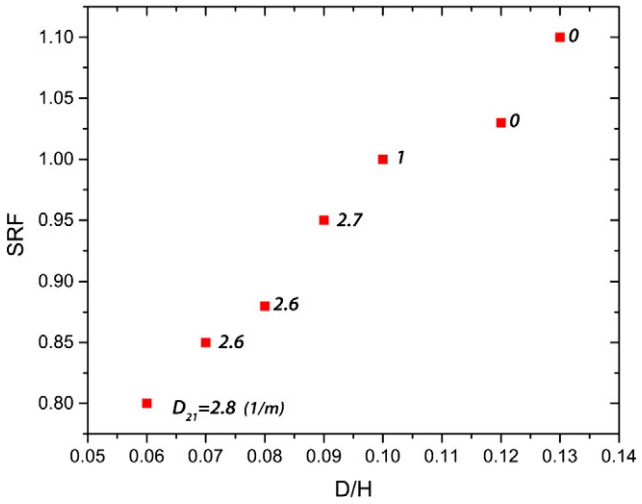

Fig. 15. Plot showing SRF values vs. D/H for different D_{21} ratios.

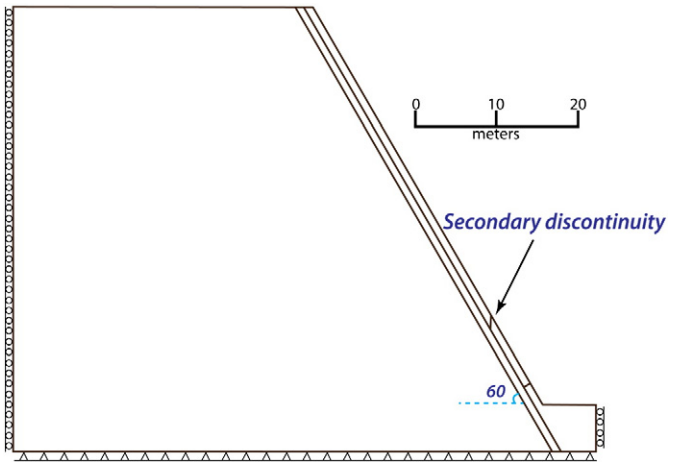

Fig. 17. Assumed geometry for FDEM + SSR simulation of ploughing failure.

it to plough under the passive slab which in turn induces fracturing at the interface between the active and passive slabs. Here the damage intensity, D_{21}, is seen to increase significantly. As the active slab continues to plough under and lifts the passive slab, the bending that develops generates tensile fractures in the middle of the slab which leads to complete failure of the footwall slope. The toe joint provides kinematic release allowing rotation of the passive slab. In the absence of a toe release joint, failure may still occur through intact rock bridge failure at the slab toe due to rotation and stress-induced fracturing of the passive slab. Fig. 19 illustrates this showing several stages of fracture development and ploughing failure. Stage 1 illustrates the base model geometry without inclusion of a toe release joint. At stage 2, tensile fracturing due to lifting of the slab results in the generation of a toe release perpendicular to the bedding. This fracture acts like the included toe release joint in Fig. 18 and provides kinematic release for rotation of the passive slab. The rest of the failure process is similar to the previous model with ploughing of the slab at stage 4 causing another fracture to develop perpendicular to the slab and leading to complete slope failure at stage 6. Thus, if there are sufficient driving forces to allow lifting up of the passive slab, ploughing failure can occur without a toe release joint through bending and tensile fracturing of the passive slab. Alejano et al. (2011) referred to this type of failure as a "partially joint controlled ploughing failure". It should be noted that D_{21} is larger for this model compared to the model with the toe joint inclusion confirming that a larger degree of damage is required to allow for kinematic release and slope failure. This is further investigated through a separate ELFEN simulation, (with identical geometry, input parameters and calculation time) but this time not allowing fracturing within the model. After about 5 cm of initial displacement, displacements cease and the model reaches equilibrium (Figure 20). Therefore, without the capability for brittle fracture, this model predicts a stable slope where in contrast the simulation with internal fracturing of the slab clearly shows failure.

To investigate the sensitivity of the ploughing failure mechanism to the dip of the secondary discontinuity, its dip angle was decreased in 5° intervals. i.e., the angle between the secondary discontinuity and

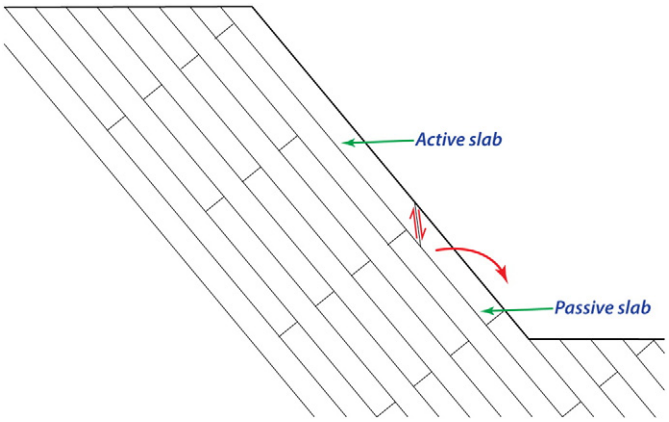

Fig. 16. Ploughing failure of footwall slopes.

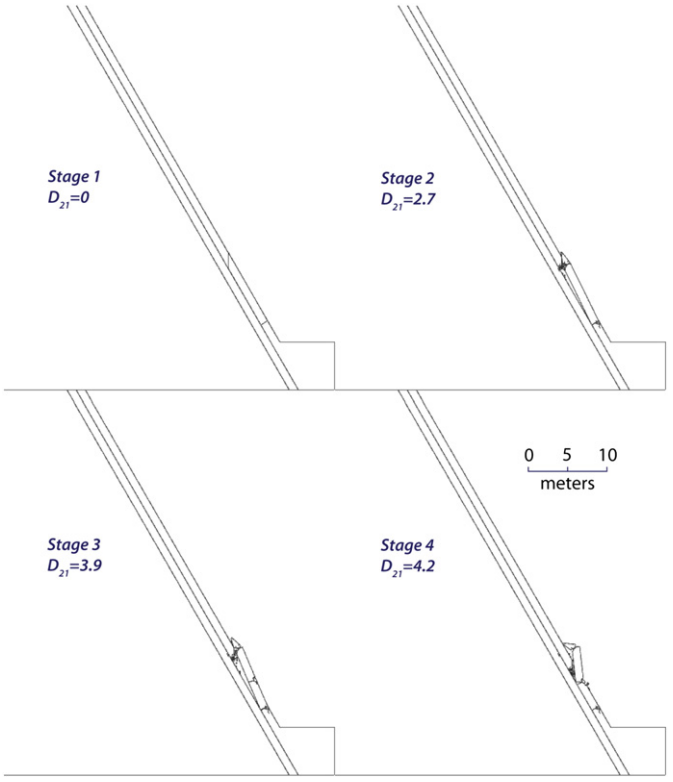

Fig. 18. ELFEN simulation of a 50 m high footwall slope showing four stages of fracture development leading to ploughing failure of the slope (with basal joint inclusion).

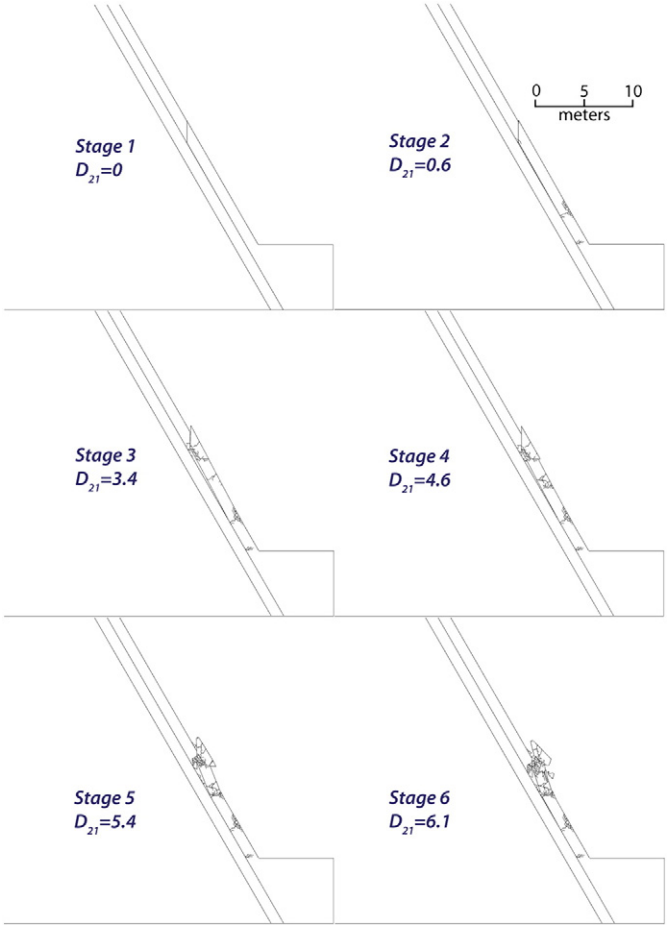

Fig. 19. ELFEN simulation of a 56 m high footwall slope showing six stages of fracture development leading to ploughing failure of the slope (without the inclusion of a basal joint).

bedding planes is increased by 5° in each model (Figure 21). Numerical modelling using ELFEN is conducted with and without the basal joint and the results are summarized in Table 6. When the dip of the secondary discontinuity is less than 80° (i.e., sub-vertical to bedding) the inclination of the joint relative to the friction angle and normal forces transmitted across the joint does not promote ploughing failure. The

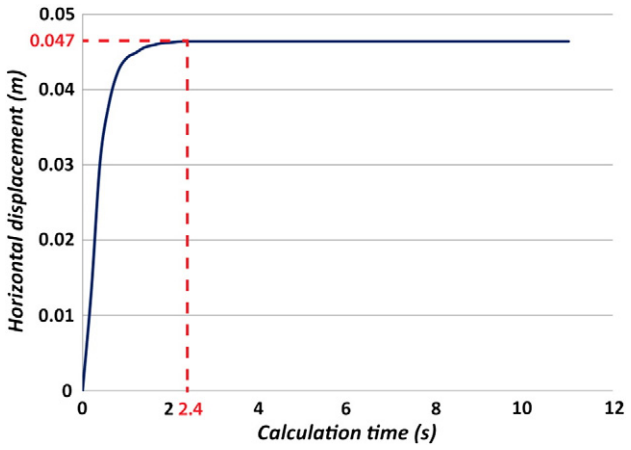

Fig. 20. Horizontal displacement vs. calculation time at the slope crest; results are obtained from simulation of partially joint controlled ploughing failure when fracturing is not allowed within the model.

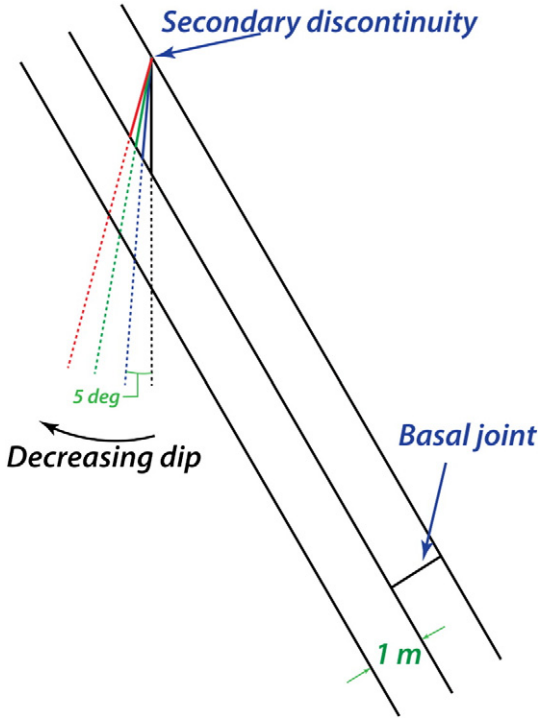

Fig. 21. Inset illustrating change in secondary discontinuity dip to evaluate the effect on the ploughing slope failure mechanism.

same results are obtained for the models without the toe joint. Hence it can be concluded that for ploughing to develop, a sub-vertical discontinuity is required at an angle that allows the driving forces of the active slab to overcome the frictional resistance and plough under the passive slab.

4.2. Controls on ploughing failure of footwall slopes

Ploughing failure in footwall slopes is strongly influenced by the engineering geology, geomechanical properties and geometry of the slope, for example slope dip and D/H ratio (Dawson et al., 1993; Stead and Eberhardt, 1997; Alejano et al., 2011). The latter were investigated with respect to the sensitivity of the model results with regard to ploughing failure.

4.2.1. Slope angle

Slope angle has a direct effect on the balance between the driving and resisting forces in footwall slopes. The ELFEN analysis was conducted for the two cases previously examined: with and without the toe release joint. A summary of the simulation results including D_{21} and SRF is presented in Table 7. The model with the toe release joint is unstable (SRF = 0.95) with a significantly lower degree of slope damage (D_{21} = 0.9) when the slope angle is decreased to 55°. The slope becomes stable with no damage with a reduction in slope angle to

Table 6
Influence of the secondary discontinuity on ploughing failure.

Model	Secondary discontinuity dip (°) -angle between bedding planes and secondary discontinuity	SRF/D_{21a} (with basal joint)	SRF/D_{21} (without basal joint)
Base model	90–30	0.75/4.2	0.8/6.1
Model 1	85–35	0.9/2.2	0.9/5.6
Model 2	80–40	1.13/0	1.15/0

Table 7
The effect of slope angle on ploughing failure of footwall slopes.

Model	Slope angle (°)	SRF/D_{21} (with basal joint)	SRF/D_{21} (without basal joint)
Base model	60	0.75/4.2	0.8/6.1
Model 1	55	0.95/0.9	1/0
Model 2	50	1.15/0	1.15/0

Table 8
Results summary of the effect of D/H ratio on ploughing failure of footwall slopes.

Model	D/H	SRF	D_{21}
Base model	0.02	0.75	4.2
Model 1	0.025	0.98	0.4
Model 2	0.03	1.05	0.4
Model 3	0.04	1.08	0

50°. The simulation results are somewhat different for the models without a toe joint. In this case the model is stable at a 55° slope angle (SRF = 1) with no slope damage ($D_{21} = 0$) emphasizing that in the absence of a toe joint, ploughing failure can only occur when enough driving forces are transferred to the passive slab to provide kinematic release through intact rock failure (as noted in the base model without a toe joint).

4.2.2. D/H ratio

Dawson et al. (1993) suggest that in general, ploughing failure in Canadian mountain coal mines is limited to slabs less than 5 m thick. At this stage of the study given the inherent instability present in the base model, the D/H ratio was increased to evaluate its effect on slope damage and the ploughing failure mechanism. Increasing D/H to 0.025 causes a significant increase in SRF, 0.98 (Table 8). A significant reduction in slope damage is also observed ($D_{21} = 0.4$) which is limited to the interface between the active and passive slabs. In model 2 displacements in order of 10 cm at the slope crest were simulated accompanied by minor fracturing at the interface between the active and passive slabs. However displacements decreased and reached equilibrium with calculation time. Model 3 did not develop intact rock fractures and was stable with negligible displacement.

5. Conclusions

The failure mechanism associated with bi-planar failure of footwall slopes where the toe breakout surface is not facilitated by a persistent discontinuity dipping out of the slope is complex. In such cases the failure mechanism involves sliding along a slope parallel discontinuity and the development of a toe breakout surface facilitated by inter block shear. Without the existence of these three surfaces, bi-planar sliding cannot occur. Within orthogonally-jointed sedimentary rock, toe breakout involves sliding along joints, failure of intact rock, and intense deformation of the slope to allow kinematic release. Footwall slope failures are common in weak, orthogonally jointed sedimentary rock. Since footwall slopes are bedded, the major principal stress may be assumed parallel to the slope face. Frictional plasticity theory is therefore a practical means to estimate the location and inclination of the inter block shear and toe breakout surface. Plasticity theory is successfully applied in this paper to explain bi-planar failure where persistent cross-cutting structures are not present to form a toe breakout and/or inter block shear surface.

Numerical simulations using a hybrid finite-/discrete-element brittle fracture approach (ELFEN) and distinct-element brittle fracture approach (UDEC Voronoi) were conducted to assess failure mechanisms associated with bi-planar failure. These models represent the first combined use of brittle fracture modelling, SSR and damage intensity measurement using FDEM techniques. Formation of an inter block shear surface in numerical modelling results demonstrated a good agreement with the prediction from plasticity theory. ELFEN and UDEC Voronoi were able to realistically simulate the interaction between existing discontinuities and intact rock bridges allowing kinematic release and failure. The results provide insights into the bi-planar footwall failure mechanism as a function of fracture initiation and propagation driven by the active–passive blocks in the slope. It is interesting to note that the modelled slope is stable when fracturing is not considered but fails when internal fracturing is allowed within the model. Similarly, ELFEN was used to simulate ploughing failure of footwall slopes with respect to the influence of toe release and secondary joints/fractures required for ploughing failure to develop.

Lastly, parametric analyses using ELFEN were conducted for both bi-planar and ploughing failure to evaluate the effect of geometrical parameters (slope angle and D/H ratio) on both bi-planar and ploughing failure mechanisms. In all the numerical models, D_{21} (a 'damage intensity' parameter), which is defined as the total length of damage to the sampling area is used along with SSR to quantitatively evaluate rock damage. The results are used to establish a better understanding of the importance of each parameter which can aid in future footwall slope design. It is suggested that the new combined FDEM and SSR/D_{21} methodology proposed in this paper has significant future application in rock slope analysis in both mining and civil applications.

References

Alejano, L.R., Ferrero, A.M., Ramírez-Oyanguren, P., Álvarez Fernández, M.I., 2011. Comparison of limit-equilibrium, numerical and physical models of wall slope stability. Int. J. Rock Mech. Min. Sci. 48 (1), 16–26.

Alzo'ubi, A.M., 2009. The Effect of Tensile Strength on the Stability of Rock Slopes. PhD Thesis University of Alberta, Edmonton, Canada.

Alzo'ubi, A., Martin, C., Cruden, D., 2007. A discrete element damage model for rock slopes. In: Eberhardt, E., Stead, D., Morrison, T. (Eds.), Rock Mechanics: Meeting Society's Challenges and Demands. Taylor & Francis, pp. 503–510.

Bahrani, N., Tannant, D.D., 2011. Field-scale assessment of effective dilation angle and peak shear displacement for a footwall slab failure surface. Int. J. Rock Mech. Min. Sci. 48 (4), 565–579.

Behrens da Franca, P.R., 1997. Analysis of Slope Stability Using Limit Equilibrium and Numerical Methods with Case Examples from the Aguas Claras Mine, Brazil. MSc Thesis Queen's University, Kingston, Canada.

Brawner, C.O., Pentz, D.L., Sharp, J.C., 1971. Stability studies of a footwall slope in layered coal deposits. 13th US Symposium on Rock MechanicsUniversity of Illinois, Urbana, United States, pp. 329–365.

Carvalho, J., Carter, T., Diederichs, M., 2007. An approach for prediction of strength and post yield behaviour for rock masses of low intact strength. In: Eberhardt, E., Stead, D., Morrison, T. (Eds.), Rock Mechanics: Meeting Society's Challenges and Demands. Taylor & Francis, pp. 277–285.

Chen, H., 1992. Appropriate model for hazard analysis in slope engineering. Sixth International Symposium on Landslides. Christchurch, New Zealand, pp. 349–354.

Cruden, D.M., Masoumzadeh, S., 1987. Accelerating creep of the slopes of a coal mine. Rock Mech. Rock. Eng. 20 (2), 123–135.

Dawson, R.F., Bagnall, A.S., Barron, K., 1993. Rock anchor support systems at Smoky River Coal Limited, Grande Cache, Alberta. 95th Annual General Meeting of the Canadian Institute of Mining, Calgary, Canada, (22 pages).

Eberhardt, E., Thuro, K., Luginbuehl, M., 2005. Slope instability mechanisms in dipping interbedded conglomerates and weathered marls—the 1999 Rufi landslide, Switzerland. Eng. Geol. 77 (1–2), 35–56.

Elmo, D., Stead, D., 2010. An integrated numerical modelling–discrete fracture network approach applied to the characterisation of rock mass strength of naturally fractured pillars. Rock Mech. Rock. Eng. 43 (1), 3–19.

Fisher, B.R., 2009. Improved Characterization and Analysis of Bi-Planar Dip Slope Failures to Limit Model and Parameter Uncertainty in the Determination of Setback Distances. PhD Thesis The University of British Columbia, Vancouver, Canada.

Fisher, B.R., Eberhardt, E., 2007. Dip slope analysis and parameter uncertainty, a case history and practical recommendations. In: Eberhardt, Erik, Stead, D., Morrison, T. (Eds.), Rock Mechanics: Meeting Society's Challenges and Demands. Taylor & Francis, pp. 871–878.

Gao, F., 2013. Simulation of Failure Mechanisms around Underground Coal Mine Openings Using Discrete Element Modelling. PhD Thesis Simon Fraser University, Burnaby, Canada.

Giani, G.P., 1992. Rock Slope Stability Analysis. Taylor & Francis.

Hamdi, P., Stead, D., Elmo, D., 2013. Numerical simulation of damage during laboratory testing on rock using a 3D-FEM/DEM approach. ARMA 2013, San Francisco, United States, 7 pages.

Hawley, P.M., Martin, D.C., Acott, C.P., 1986. Failure mechanics and design considerations for footwall slopes. CIM Bull. 47–53.

Hoek, E., Bray, J., 1981. Rock Slope Engineering. E & FN Spon.

Hoek, E., Brown, E.T., 1997. Practical estimates of rock mass strength. Int. J. Rock Mech. Min. Sci. 34 (8), 1165–1186.

Hoek, E., Carranza-Torres, C., Corkum, B., 2002. Hoek–Brown failure criterion. North American Rock Mechanics Symposium, Toronto, Canada, (7 pages).
Itasca, 2010. Slope Model, Description of Formulation with Verification and Example Problems. Revision 2. Itasca Consulting Group Inc., Minneapolis, United States.
Itasca, 2012. UDEC 5.0. Manual. Itasca Consulting Group Inc., Minneapolis, United States.
J.E.Jennings, J.E., 1970. A mathematical theory for the calculation of the stability of slopes in open cast minesProceedings of Planning of Open Pit Mines. Johannesburg, South Africa, pp. 87–102.
Jin, X., Mingdong, C., Tianbin, L., Lansheng, W., 1992. Geomechanical simulation of rockmass deformation and failure on a high dip slope. Sixth International Symposium on Landslides. Christchurch, New Zealand, pp. 349–354.
Kazerani, T., Zhao, J., 2010. Micromechanical parameters in bonded particle method for modelling of brittle material failure. Int. J. Numer. Anal. Methods Geomech. 34 (18), 1877–1895.
Konietzky, H., 2004. Numerical modelling of discrete materials in geotechnical engineering, civil engineering and earth sciences. Proceedings of the First International UDEC/3DEC Symposium. Taylor & Francis, Bochum, Germany (29 September–1 October 2004).
Kvapil, R., Clews, M., 1979. An examination of the Prandtl mechanism in large dimension slope failures. Trans. Inst. Min. Metall. A 88, A1–A5.
Lajtai, E.Z., 1969. Shear strength of weakness planes in rock. Int. J. Rock Mech. Min. Sci. Geomech. Abstr. 6 (5), 499–515.
Li, T.B., Xu, J., Wang, L.S., 1992. Ways and methods for the physical simulation of landslide. Sixth International Symposium on Landslides. Christchurch, New Zealand, pp. 487–491.
Nathanail, C.P., 1996. Kinematic analysis of active/passive wedge failure using stereographic projection. Int. J. Rock Mech. Min. Sci. Geomech. Abstr. 33 (4), 405–407.
Rockfield, 2009. ELFEN manual version 4.4. Rockfield Software Limited, Swansea, UK.
M.J.Scoble, M.J., 1981. Studies of Ground deformation in British Surface Coal Mines. PhD Thesis University of Nottingham, Nottingham, UK.
D.Stead, D., E.Eberhardt, E., 1997. Developments in the analysis of footwall slopes in surface coal mining. Eng. Geol. 46 (1), 41–61.
Stead, D., Eberhardt, E., Coggan, J.S., 2006. Developments in the characterization of complex rock slope deformation and failure using numerical modelling techniques. Eng. Geol. 83 (1–3), 217–235.
Stimpson, B., Robinson, K.E., 1982. A computer program for footwall slope stability analysis in steeply dipping bedded deposits. 3rd Conference on Stability in Surface Mining, pp. 437–455.
Tannant, D., LeBreton, R., 2007. Footwall slope slab failure at a mountain coal mine. In: Eberhardt, E., Stead, D., Morrison, T. (Eds.), Rock Mechanics: Meeting Society's Challenges and Demands. Taylor & Francis, Vancouver, Canada, pp. 1263–1270.
Tuckey, Z., Stead, D., Havaej, M., Gao, F., Sturzenegger, M., 2012. Towards an integrated field mapping-numerical modelling approach for characterising discontinuity persistence and intact rock bridges in large open pits. The Canadian Geotechnical Society (Geo Manitoba), Winnipeg Manitoba, (15 pages).
Vyazmensky, A., Elmo, D., Stead, D., 2010. Role of rock mass fabric and faulting in the development of block caving induced surface subsidence. Rock Mech. Rock. Eng. 43 (5), 533–556.
Wang, L., Zhang, Z., Cheng, M., Xu, J., Li, T., Dong, X., 1992. Suggestion on the systematical classification for slope deformation and failure; landslides–glissements de terrain. Sixth International Symposium on Landslides. Christchurch, New Zealand, pp. 1869–1877.
Yan, M., 2008. Numerical Modelling of Brittle Fracture and Step-Path Failure: From Laboratory to Rock Slope Scale. Simon Fraser University, Burnaby, Canada. PhD Thesis.